COMPDYN 2021
8th ECCOMAS Thematic Conference on
Computational Methods in Structural Dynamics and Earthquake Engineering
M. Papadrakakis, M. Fragiadakis (eds.)
Streamed from Athens, Greece, 27–30 June 2021

GRAPHICAL METHODS, KINEMATIC AND FINITE ELEMENT ANALYSIS OF THE PREMILCUORE MASONRY BRIDGE

Linda Giresini[1], Daniela De Paola[2], Mario Lucio Puppio[3,*] and Giovanni Buratti[1]

[1] Department of Civil and Industrial Engineering
Largo Lucio Lazzarino, 1, 56100 Pisa (Italy)
linda.giresini@unipi.it, giovanni.buratti.2707@gmail.com

[2] Project Engineer
Pisa (Italy)
depaola.daniela@gmail.com

[3] Department of Civil, Environmental Engineering and Architecture
Via Marengo, 2, 09123 Cagliari (Italy)
mariol.puppio@unica.it

*corresponding Author

Abstract

This paper presents the results of static and seismic vulnerability analyses performed on a single-span masonry bridge located in Northern Italy. The structure, dated back to the 17th century, is a bridge with single-span of about 16 meters and height of 8 meters, built with rubble and irregular masonry. A preliminary static analysis was performed on the bridge through traditional graphic approaches such as the Méry's rule and the Durand-Claye's method. Afterwards, a kinematic non-linear analysis was executed once the collapse mechanism under horizontal earthquake-type actions was identified. Finally, a static finite element analysis with brick elements was performed to state the seismic vulnerability of the bridge, by changing its mechanical properties to evaluate their influence on the structural response. Collapse load factors have been also computed considering non-uniform gravitational loads and horizontal settlements at the bridge foundations.

Keywords: masonry bridge, graphical methods, plastic hinge, arch bridge, seismic vulnerability; pushover analysis.

1 INTRODUCTION

Masonry Arch Bridges (MAB) represent a considerable portion of the ancient road infrastructures. The main characteristics of this artwork is a massive structure with significant stiffness and resistance. This aspect allows these infrastructures being less prone to vibration and deformation with respect to the modern structures. Furthermore, masonry bridges, as other historical structures, are characterized by a significant durability that permits their survival over the centuries.

MAB have an ancient origin. The first application of masonry in river overpasses are probably abutments and architraves of elementary bridges, made by simply supported wooden decks. The diffusion of arches in Mesopotamia and in Egypt gave a significant impulse to their use. The first stone arch can be dated back to the 4th millennium BC. Here the substitution of a previous slab made of intertwined reeds with dry stones and sun-dried bricks created the first documented arch of the history.

The first MAB was probably built in China, in the 3rd millennium BC. Later the Romans, famous road builders, massively used arches for the construction of bridges and aqueducts, some of which still survive nowadays [1].

For what concerns the computational modelling of MAB, from simplified methods to complex nonlinear finite element or discrete elements, interesting contributions can be found in [2–4]. For a proper computational modelling, the definition of geometry and mechanical properties of MAB is essential. In [5], the significant role of geometrical and mechanical parameters like arch thickness and filling is highlighted. In the same paper, a geometrical survey of 59 segmental MABs located in Portugal and Spain is reported. Thus, an accurate geometrical and mechanical survey is crucial in the safety evaluation; modern techniques can be very precious in this sense [6], especially when the internal core is not accessible. Specific techniques can be applied to limit the uncertainties in the composition of internal cores [7, 8]. When performing a structural assessment, it is important to vary the masonry and soil mechanical properties in case of uncertainties in their definition [9]. Sensitivity analyses are then often proposed to investigate the impact of the most important parameters such as the tensile strength of masonry [10–12]. Moreover, when dealing with uncertainties, it could be relevant to perform probabilistic analysis. For example, Casas [13] proposes a probabilistic assessment of MAB at the Serviceability and Ultimate Limit States. This work also illustrates recurring failure modes: four-hinge mechanism, the ring separation in multi-ring arches and the slippage at the foundations. In [14] a simplified approach is proposed for the evaluation of fragility curves of MAB in case of seismic action. The study is carried out on numerous structures and broadened to a stock of roadway and railway bridge networks in dangerous condition to provide stakeholders a management tool.

There are diverse methodologies to study the static and the dynamic behavior of MAB. Very interesting graphical and numerical methods were developed in the past (from the 18th century) to study the static behavior of arch, in particular from the French Engineering Grand Écoles. This paper has the aim of performing all the possible analysis methods usually performed for MAB and of proposing qualitative comparisons.

In Section 2 a review of traditional and modern techniques is presented and applied to a representative case of study. The MAB selected for the investigation, reported in Section 3, is the *Premilcuore bridge* located in the District of Forlì-Cesena, Central Italy. The graphical methods and the numerical analyses are illustrated in Section 4.

2 BACKGROUND

2.1 Traditional graphical methods

In order to carry out a first simplified study of the stability of the vault, two different traditional methods have been employed: the so-called Mèry's Rule and Durand-Claye's Method.

Mèry's Rule, to which the credit for formalising the concept of thrust line is attributed, has risen to fame in the technical field particularly thanks to its ease of application. Indeed, it is interesting to observe how it is the only method still quoted in today's textbooks. Even though it was based on arbitrary assumptions [15], this method was applied for over a century for the design of arches and vaults. The foundation of this procedure is the personal criterium according to which the ideal condition for the arch can be identified by a thrust line that is entirely contained in the area defined by the middle third of the sections, intending to guarantee that the latter are completely reactive and the arch is not subjected to failure.

In accordance with Méry's studies, among the infinite curves of this type, which are able to ensure the arch equilibrium, the definition of the design line relies on the hypothesis that this thrust line passes through three pre-defined points: the lower middle third of the two sections in close proximity to the springers and the upper middle third in the keystone, where the direction of normal force is horizontal, according to the premise of symmetry of the applied load.

The second method, which is a more refined form the theoretical point of view, is the one studied by Durand-Claye. It was conceived as a method to assess the stability of a symmetrical arch, symmetrically loaded by vertical forces under the condition that the material has finite value of the compressive strength and that it has a negligible tensile resistance.

This method essentially consists in defining the set of all the possible values of the internal forces in the keystone, the normal force N and the bending moment M, or, alternatively, the normal force and its eccentricity in relation to the axis curve, which ensure equilibrium and are compatible with the material strength. According to the assumptions, through each cross-section, possibly partialized, the compressive stresses vary with a linear law. The result of this procedure gives the graphical representation of the envelope of the aforementioned forces.

This method, unlike the previous one, allows to identify all the possible thrust lines capable of ensuring the balance in compliance with the limits of the material strength. Its value resides in checking the existence of admissible solutions without requiring to find the true one, which could be reached only by bringing into play the elastic properties of the material and the compatibility conditions. Assuming that the true solution exists, it is definitely included among these ones.

The Durand-Claye's method does not require either special hypotheses regarding the shape of the thrust line or regarding a predefined position of rupture joints, allowing to obtain several advantages. In particular, it allows to evaluate the degree of safety of the arch, the possible trend of the thrust line and the identification of the most stressed sections of the structure. This method is well suited to various types of arches, having different geometries and made with different materials.

2.2 Rigid block and arch models for kinematic analyses

A more modern approach to investigate the structural behavior of masonry buildings and bridges refers to limit analysis and non-linear dynamic analysis of rigid block models. Often, masonry structures - and especially historic constructions - can be regarded as composed by structurally independent parts or rigid blocks connected by ideal hinges. This occurs particularly when the connections between vertical members and between horizontal dia-

phragms/roof and walls are not effective [16]. In order to avoid such an undesirable behavior, tie-rods [17, 18], fiber composite stripes [19, 20] and strength anchors [21, 22] of suitable characteristics can be used. An extensive review on kinematic and rocking approaches for monolithic masonry walls, specifically regarded as rigid blocks on rigid foundations is reported in [23]. Among the methodologies based on limit analysis, recently many contributions were proposed considering the frictional forces [24–29] playing a crucial role in the assessment of the mechanism evolution. Evidently, these frictional forces should be determined through proper experimental testing [30]. Among the methods based on non-linear dynamic MAB (rocking) analysis, there exist models of walls connected with different types of horizontal diaphragms [31], but also of the corner mechanism as typical out-of-plane mode of masonry buildings [32]. A comparative study between the kinematic and non-linear dynamic methods investigating the 3D corner failure mechanism, also considering the thrusting roof and the stabilizing contribution of frictional resistances exerted within interlocked walls, is reported in [33]. One of the main issues arisen in these analyses is the output variability observed when input and boundary conditions change. Thus, probabilistic approaches suitable to describe the behavior of rocking structures have been defined [34, 35]. Moreover, rocking can be also seen as seismic dissipation technique for slender structures [36] and masonry walls [37]. Referring to arch-type structures, the rocking arch model assumes rigid blocks and rigid supports and is therefore only dependent on geometric properties similarly to the rocking block model. The susceptibility of masonry arches to earthquake loading is analytically and experimentally evaluated in [38] where the rocking arch model is a four-hinge mechanism.
However, the approach currently most used in the professional practice for rigid block models is the kinematic analysis based on the displacement-based method. In it, the capacity in terms of both forces and displacements is compared with the seismic demand through the construction of acceleration-displacement response spectra. The standards from different countries (e.g. New Zealand [22] and Italy [39]) give specific indications about the way of calculating the collapse multipliers for each collapse mechanism and the methods to assess the seismic vulnerability through the acceleration-displacement curves. The *Premilcuore* bridge is here analyzed considering different single degree of freedom four-hinge mechanisms originated by different positions of the ideal hinges along the arch. The first aim of the kinematic analysis is to identify the most probable collapse mechanism, which corresponds to the lowest collapse multiplier according to the kinematic theorem of the limit analysis. Afterwards, the capacity curve is computed by following the Italian standards [40] and the safety verification is made through a kinematic non-linear analysis, namely by comparing the displacement demand with the displacement capacity.

2.3 Finite element and discrete element models

More refined approaches model masonry structures using micro and macro-modelling techniques. The formers separately consider the mechanical properties of the single components (bricks/blocks and mortar joints); the latter use simplified elements with homogenized properties. A consolidated model is represented by discrete macro-elements able to reproduce typical failures of masonry walls [41, 42]. A comparison between discrete macro-element and rigid block models used to assess the seismic vulnerability of a church façade is presented in [43]. An alternative method to discrete macro-element models regards the well-known finite element models, where masonry is modelled by means of planar (shell-plate type) or tridimensional (brick) elements with homogenized mechanical properties. A crucial issue of this modelling strategy consists in the correct selection of the masonry non-linear constitutive law and of the domain failure. These models offer a wide range of output, in terms of stress, strain, displacement, forces and energy [44], which have to be properly treated. Recently, some au-

thors developed discrete element models for the structural analysis of bridges [45, 46], whereas refined finite element models of multi-span masonry bridges were proposed in [47] performing nonlinear static, nonlinear dynamic, and incremental dynamic analyses under 14 earthquake records. This paper proposes the modeling of the *Premilcuore* bridge through a finite element model made of brick elements, whose features are illustrated in Section 3.2. The different modelling and analysis procedures, including the graphical methods and the kinematic analyses, are then discussed analogously to what is done in [48] in Section 5.

3 CASE OF STUDY

3.1 Geometry and masonry type

The *Ponte Nuovo (New Bridge)* of *Premilcuore* is named from the rebuilding (in 1650-1656) of a previous roman bridge, probably dated to the 2nd century AD [49]. The reconstruction of the New Bridge (Figure 1) was made after the collapse of the previous one, whose right abutment was kept (Figure 2a). The infrastructure is placed along the historical Florentine roads, which connected the two Italian regions Tuscany and Emilia Romagna across the *Rabbi* stream.

Figure 1: Aerial view of the bridge

The structure is characterized by a segmental arch with a length of 15.90 m and a maximum rise of 4.35 m. The deck is built with a "donkey back" shape with a slope of the ramp of about 22 degrees according to the canons of the medieval period.
The masonry of the abutments, of the wing walls and of the parapets is made of irregular stones except for the ring stone and the lower part of the abutment, which is built with regular stone. The river-bed appears irregular and the lithotype of the foundation has a predominant rock component. A large cracking under the bridge highlights a hypogea cavity that collects the runoff water.
The three metallic ties that appear under the arch (Figure 2b) are installed in the 1930's, after some seismic events that affected the area producing damages in the adjacent building (1818-1819).

(a) (b)

Figure 2: Details of the bridge: wing wall (a) and intrados (b)

3.2 Assumptions of the analysis

A detailed survey of the geometry is carried out according to [50]. A literary review allowed to define a part of the geometry that was not directly measured on site, by means of the design criteria used when the reconstruction took place [15, 51, 52]. The extension of the abutment and the thickness of the arch are in line with the 17th century design rules.

At the time of the construction of *Premilcuore bridge* there was no technical distinction between the part of the backfill that had or not a static rule in the bridge conception, so all the filling placed over the masonry vault is considered as non-structural [1, 53].

An identification of the mechanical properties of the bridge is carried out according to [54, 55]. The material variability, in existing buildings, is considered to be one of the most significant causes of uncertainties particularly affecting the structural response [56–58]. To consider the uncertainties in masonry properties a sensitivity analysis is carried out considering a variation of the mechanical properties in the range ± 40% with respect to the average values reported in Table 1. The tensile strength is assumed to be 1/10 of the compressive strength.

The Max Stress criterion, also known as *Galileo-Rankine's criterion*, was assumed in the analysis.

Material	Elements	c [MPa]	φ [Deg]	E [MPa]
1	Vaults, spandrel walls	0.253	54.9	975
2	Arch ring, abutment	0.411	54.9	1320
3	Backfill	0.05	21.8	500

Table 1: Mechanical properties of the bridge components.

For all the elements a uniform specific weight of 18 kN/m^3 is assumed. The live load assumed is a distributed load of 5 kN/m^2; this value is indicated in [59] and in CNR Guidelines [60] for the masonry carter bridges of the 19th and 20th century and represents the same value that is currently used for the design of a pedestrian footbridge.

3.3 Finite element model

A tridimensional model of the central segment of the bridges is implemented in the software Straus 7 (r2.3.3). The model is composed by 8242 nodes, 7908 brick and 288 beam elements (Figure 3). The beam properties are *cut-off bars* with no tensile strength to model the interface with the soil foundation. The parapets are modelled as *non-structural masses*.
The material properties of Table 1 are assigned to the different parts of the bridge. In Magenta the material 1, in Yellow the material 2 and in Cyan the material 3 (Figure 3).
The lateral portions of the abutments adjacent to the soil of the access ramp (parallel to plane y-z) are restrained only in x-direction. The nodes under the foundations (parallel to plane x-y) are completely fixed.

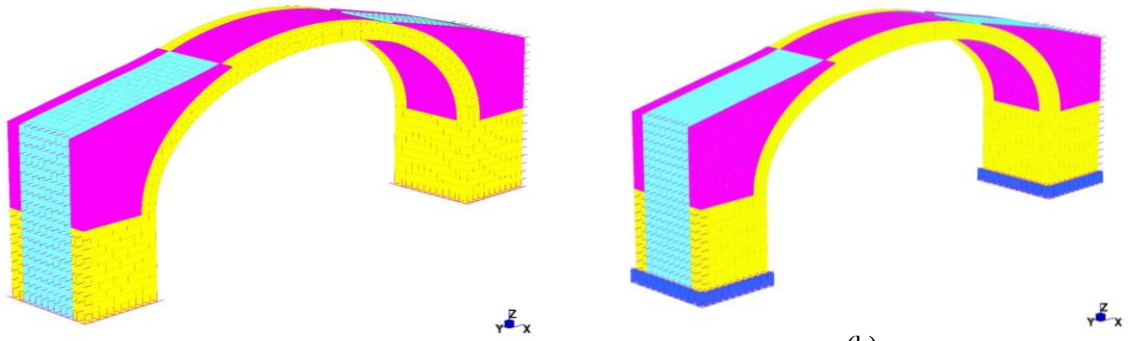

(a) (b)

Figure 3: Three-dim model, for Static (a) and Seismic (b) analysis.

4 ANALYSIS OF THE PREMILCUORE BRIDGE

4.1 Traditional / Graphical methods

In order to assess the stability of the arch, the Mery's Rule has been firstly applied. Preliminarily, the arch between the springer and the keystone has been divided into ten voussoirs with the same length, Δs. Then, the study has been focused on the section of the arch between the intermediate rupture joint and the keystone. In accordance with well-established assumptions [51], the lower section can be located halfway, in terms of height, between the springing line and the highest point of the intrados, meaning between the voussoirs 7 and 8.
Self-weight and traffic loads have been considered, and the latter has been schematized as a uniform load acting longitudinally along the entire bridge. Its intensity was set equal to 5 kN/m^2. The different loads acting on each element of the structure are shown in Table 2.

	Specific weight γ = 18 kN/m^3				Equivalent Traffic Load q_k = 5 kN/m^2		Resultant Force
Voussoirs	Voussoirs Self-Weight Load	Filling Load	Parapet of the bridge Load	Resultant Load	Length of the vous-soirs	Traffic load	R
	[kN]	[kN]	[kN]	[kN]	[kN]	[kN]	[kN]
1	45.4	0.0	12.8	58.2	106.3	15.4	73.6

2	45.4	0.0	11.0	56.4	105.4	15.3	71.7
3	45.4	0.0	10.6	56.0	104.3	15.1	71.1
4	45.4	1.8	10.9	58.1	102.8	14.9	73.0
5	45.4	9.8	11.1	66.4	100.1	14.5	80.9
6	45.4	24.0	11.1	80.5	95.9	13.9	94.4
7	45.4	43.5	10.7	99.6	89.2	12.9	112.5
8	45.4	64.7	9.7	119.9	77.6	11.3	131.1
9	45.4	74.7	7.4	127.5	56.9	8.3	135.7
10	45.4	41.0	2.9	89.4	20.9	3.0	92.4
						Total	936.4

Table 2 – Discretization of the Arch.

Applying the loads on each segment, the funicular polygon passing through the upper middle third of the keystone and the lower middle third of the previously mentioned section has been drawn. Thus, the thrust line of the arch has been graphically obtained, together with the magnitude of the forces at the extremities, H and S (Figure 4).

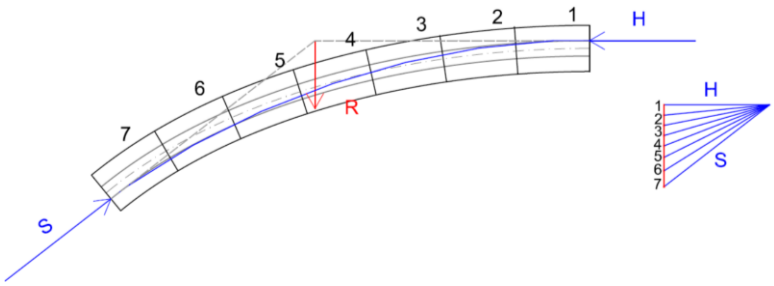

Figure 4: Thrust line according to Mery's Rule.

Subsequently, with the purpose of assessing in a different way the stability property of the vault, the Durand-Claye's method has been applied. The arch has been schematized in the same way, with ten voussoirs between the springer section and the keystone. The same loads have also been considered (Figure 5).

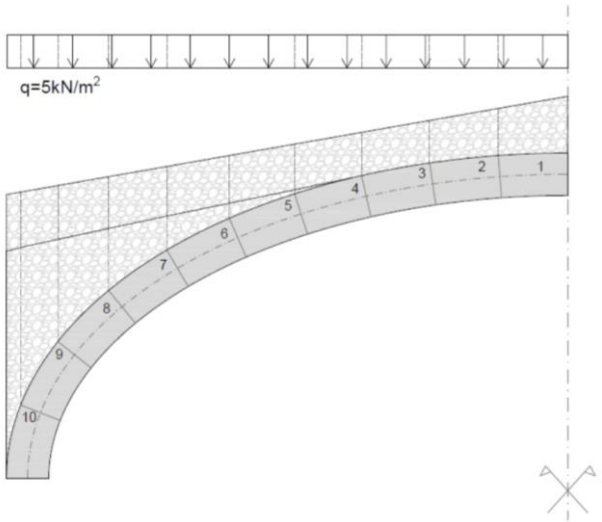

Figure 5: Mechanical model for the arch – Durand-Claye's method.

The rectangular cross section has a width of 3.65 m and a height of 0.65 m. The resistance of the material was evaluated considering the average value referred to the various parts of the structure; it has been assumed equal to f_c=2.10 MPa.
By applying the Durand-Claye's method for three different control sections, the same number of areas of stability at the keystone have been identified (Figure 6), hence, their intersection has been found (Figure 7).

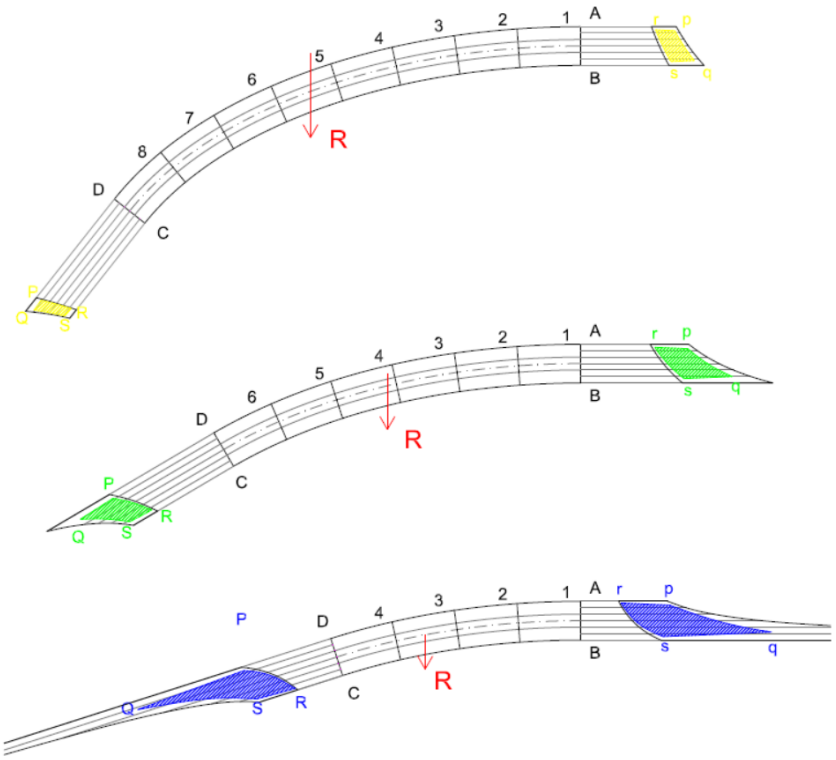

Figure 6: Durand-Claye's stability areas

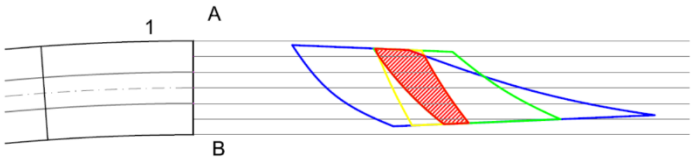

Figure 7: Intersection among the stability areas

The thrust lines corresponding to the four vertices of the stability curve identify the area within in which the actual pressure thrust will be included. The latter satisfies the conditions of balance and strength of the material. Each line can be associated with the value of the force acting on the arch (Figure 8). The arch is more vulnerable where the area containing the pressure curve is outside the middle third of the section.
Having identified the solutions related to the two simplified methods, Mery and Durand-Claye, their comparison shows that the values obtained using the Mèry's rule fall within the range identified with the Durand-Claye's method, as expected (Figure 9).

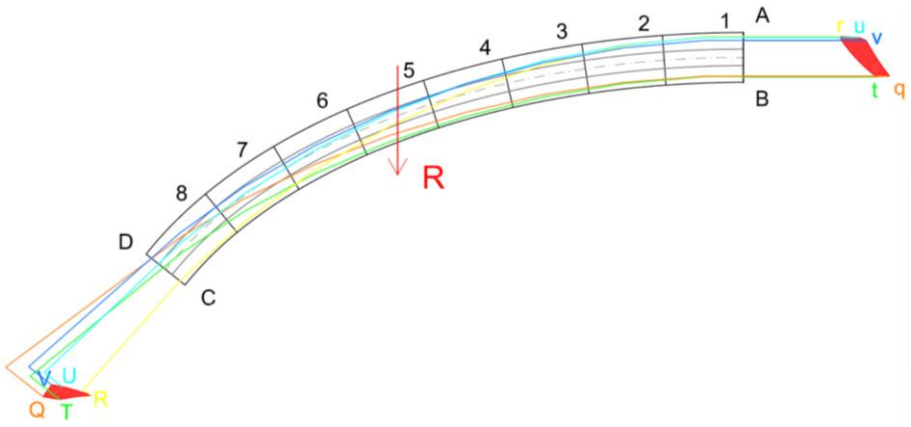

Figure 8: Thrust line according to Durand-Claye's Method.

.

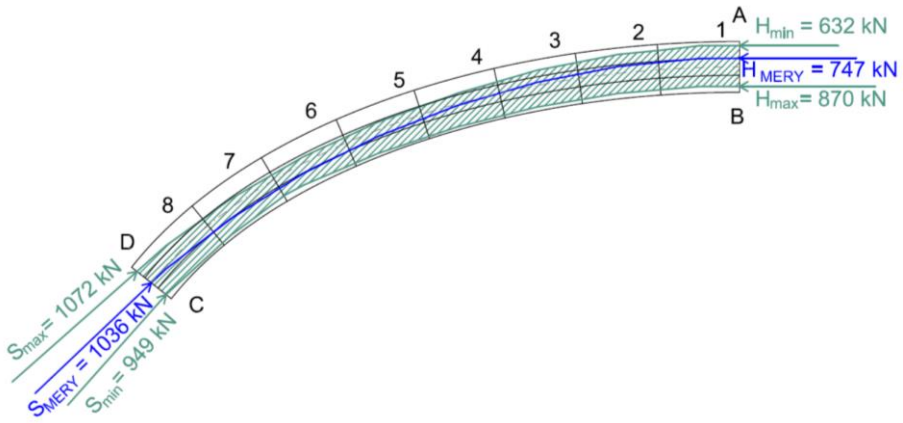

Figure 9: Comparison between Méry's and Durand-Claye's graphical solution

4.2 Identification of the collapse mechanism and non-linear kinematic analysis

Let us assume that the single span bridge is made of rigid blocks whose contact surfaces have null tensile strength, infinite compressive strength and sliding impeded. These three conditions are the well-known Heyman's hypotheses [53]. From a static point of view, the bridge is subjected to its self-weight and to the permanent loads of backfill and bridge deck with parapets. According to the Heyman's safe theorem, "if a line of thrust can be found which is in equilibrium with the external loads and which lies wholly within the masonry, then the structure is safe". The rigid block analysis is aimed at assessing the seismic vulnerability of the bridge arch and consists in two steps:

1) identification of the more likely failure (four-hinge) mechanism;
2) non-linear kinematic analysis in which the displacement capacity is compared to the displacement demand.

When the seismic action is considered, the arch is subjected to inertial forces which modify the line of thrust. The distribution of inertial forces q_i is not unique as the interaction between arch and backfill is complex. Four possible models, schematically displayed in Figure 10 considering a horizontal ground acceleration from right to left, are considered [61]:

- (M1): only the sub-blocks of the left semi-arch are subjected to the inertial force q_i, equal to the horizontal acceleration multiplied by the mass of the block itself and that

of the tributary individual horizontal strip of the backfill included between the extrados and the vertical line passing from the corresponding arch springer. The semi-arch on the right is not interested by inertial forces as here the backfill is supposed to be detached from the extrados.

- (M2): analogous to (M1), but with the sub-blocks of the semi-arch on the right subjected to the inertial force q_i;
- (M3): each sub-block is subjected to a horizontal force equal to the gravitational load that it is bearing;
- (M4): the inertial forces applied as uniform horizontal load only act on the semi-arch on the right. The resulting force of q_h is equal to the total vertical load (self-weight and backfill weight).

Considering all four models, the process to identify the four-hinge mechanism is iterative. Firstly, an attempt position of the four hinge is assumed considering only the arch since the bridge piles are stocky (Figure 10). The principle of virtual work allows calculating the collapse multiplier α by dividing the external work made by the vertical forces with that made by the horizontal forces. Once α is calculated, the reaction and internal forces between each sub-block are computed and the line of thrust, passing through the assumed hinges, can be drawn. If this line of thrust lies wholly within the masonry, α is also a statically admissible multiplier according to the limit analysis theorem and therefore the actual collapse multiplier. Otherwise, the procedure should be repeated by moving the hinges where the eccentricity (given by the ratio of bending moment to normal force on each block) is maximum, up to the condition for which the line of thrust lies wholly within the masonry. M4-m2-m3-m1

Comparing the results obtained by applying this procedure, (M1) and (M4) provide the highest and lowest estimation of the collapse multiplier respectively. (M3) corresponds to a collapse multiplier between that of (M1) and (M2). The most conservative model is therefore (M4) but the assumption of a constant horizontal load (Figure 10) is not fully realistic. On the contrary, (M3) is the simplest model and, as already illustrated in [61], can be accepted for a reliable estimation of the collapse multiplier.

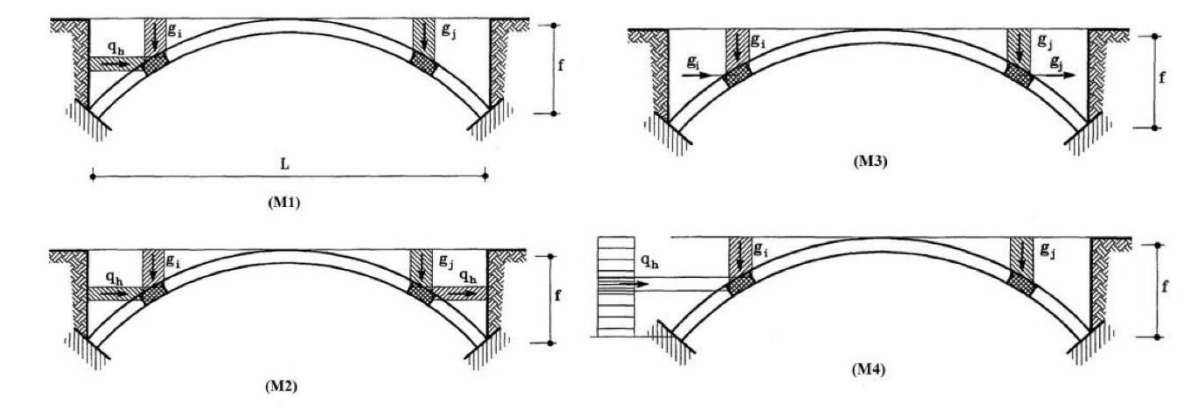

Figure 10: Models with different distribution of inertial forces (from [61]).

Its collapse multiplier is close to that of M1 and therefore such a different assumption does not markedly change the final result. For these reasons, model (M3) is considered in the following calculations. By performing the described iterative procedure, the eccentricity trend

shown in Figure 11.a is obtained at the third attempt and the corresponding deformed shape is displayed in Figure 11.b.

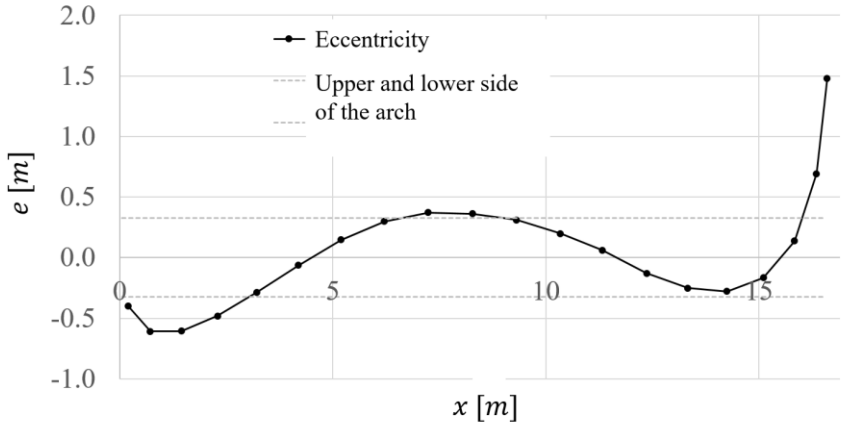

(a)

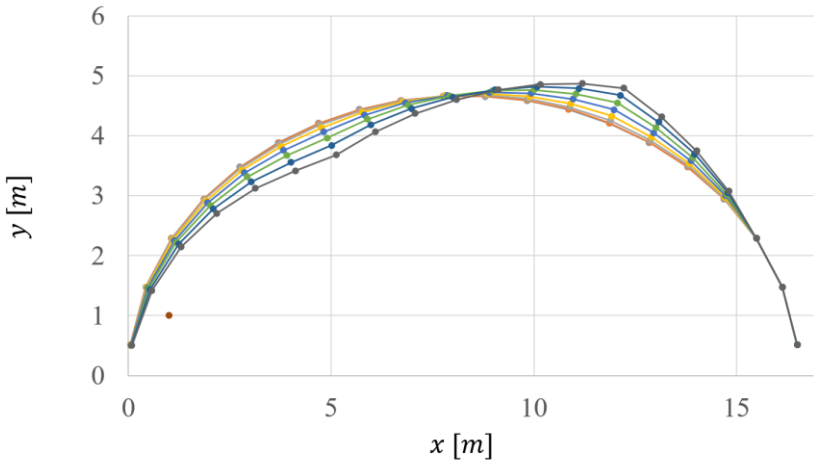

(b)

Figure 11: Eccentricity of the line of thrust obtained with the third attempt of hinge position change (a); evolution of deformed shape in the construction of the acceleration-displacement curve (b).

For this collapse mechanism, the capacity curve is firstly drawn by monotonically increasing the rotational angles between the rigid blocks constituting the arch. The displacements in x and y directions can be calculated through trivial geometric considerations from these rotational angles. This results in a progressive change of the deformed shape visible in Figure 11.b. The capacity curve is obtained by calculating through the principle of virtual work the acceleration corresponding to each imposed displacement (black curve of Figure 12).
The control point is selected as the center of mass of the key-stone and the confidence factor required to compute the acceleration is $CF = 1.35$ [40]. The ultimate displacement, corresponding to the zero acceleration capacity, is (Figure 12):

$$d_0 = S_{d,0} = 8.90\ cm \quad (1)$$

And the corresponding displacement capacity d_{ULS} is, for the ultimate limit state ULS [40]:

$$d_{ULS} = 0.4 \times S_{d,0} = 3.56\ cm \quad (2)$$

The displacement demand has to be computed by considering the secant period T_{SL} corresponding to the ultimate limit state from the expression found in the Italian standards [40]:

$$T_{SL} = 1.68\pi \sqrt{\frac{d_{ULS}}{a(d_{ULS})}} = 0.62\ s \tag{3}$$

The intersection between the dotted line of Figure 3 identified by T_{SL} and the elastic acceleration demand response spectrum (ADRS) gives the displacement demand:

$$S_d(T_{SL}) = 2.01\ cm \tag{4}$$

to compare with the displacement capacity. The verification is satisfied, being the capacity higher than the demand:

$$d_{ULS} = 3.56\ cm > S_d(T_{SL}) = 2.01\ cm \tag{5}$$

Resulting in a safety factor SF of:

$$SF = \frac{d_{ULS}}{S_d(T_{SLV})} = \frac{3.56}{2.01} = 1.77 > 1. \tag{6}$$

The bridge therefore results in a safe condition, which results even safer by considering a design ADRS with a behavior factor q [39]. This aspect confirms that these arches are rarely vulnerable to such mechanism, as already discussed in [61].

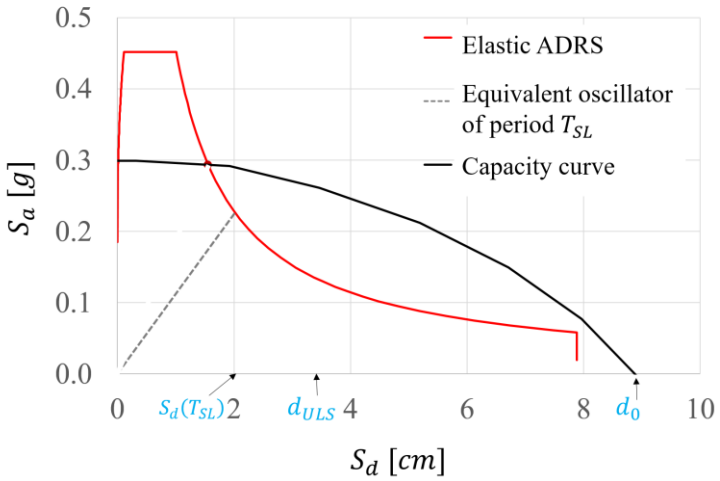

Figure 12: Seismic vulnerability assessment through non-linear kinematic analysis.

4.3 FEM analysis

4.3.1. Nonlinear static analysis (gravitational loads)

Nonlinear static analysis is carried out considering both symmetric and asymmetric incremental live loads. The gravitational load is applied into the two first steps. After that, an increasing live load is applied to identify the collapse multiplier (λ) with respect to 5 kN/m^2. The collapse is identified considering the numerical divergencies of the model. In Figure 13 and in Figure 14 the maximum principal stresses are displayed. The collapse multipliers λ are illustrated in Table 3. The bridge is safe with respect to the static live load, also considering a non-uniform distribution, and the worse resistance for masonry.

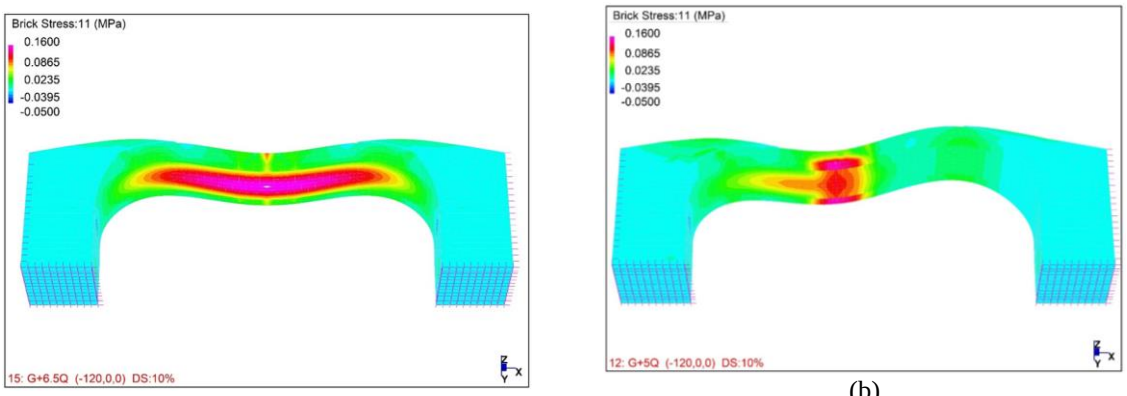

(a) (b)

Figure 13: Contour of σ_{11} in case of symmetric (a) and asymmetric live load (b).

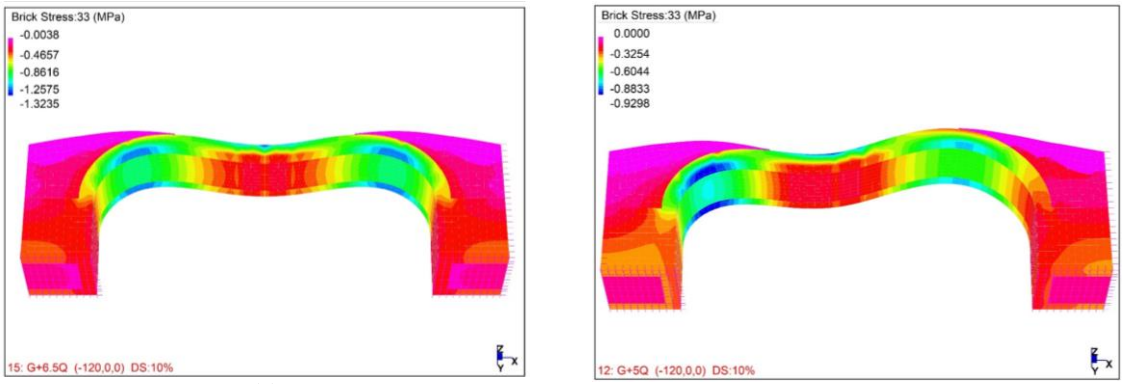

(a) (b)

Figure 14: Contour of σ_{33} in case of symmetric (a) and asymmetric live load (b).

Material	$\lambda_{uniform}$	$\lambda_{non\text{-}uniform}$
Average – 40%	4.0	4.5
Average	6.5	5.0
Average + 40%	9.0	6.0

Table 3: Collapse multiplier for static analysis.

4.3.1. Nonlinear static analysis (seismic actions)

A seismic push-over analysis is performed on the model of Figure 3 (b). The analysis is set applying first the gravitational load and after introducing the seismic action in transverse direction (Y-direction in Figure 3). The transverse direction is chosen since kinematic analyses are performed in the longitudinal section of the arch. The effect of transverse ties is neglected for the sake of safety.

The pushover curves are shown in Figure 15, considering the control displacement of a node in the middle of the arch (node 716). In these curves, the ultimate displacement depends on the material quality. It is interesting to highlight that all the curves end up at V_b=1585 kN that corresponds to a shear value of about the 90 % of the design seismic action. The overturning (joined to a crushing of masonry at the foundation) is the cause of this behavior. The hypothesis of smooth constraints (without friction) on the lateral face of the bridge consents the global

overturning. The analysis, made this prudential assumption, shows a good performance of the structure with respect to transverse action. This result is in line with the main indication in literature, which considers the kinematic approach as the most interesting for MAB.

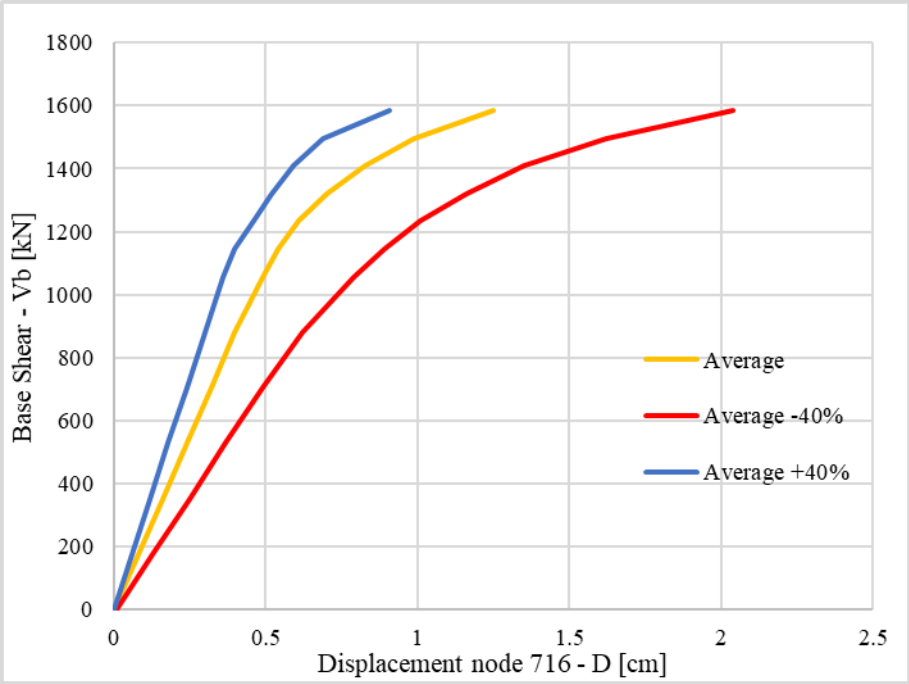

Figure 15 – Capacity curves.

5 CONCLUSIONS

The presence work dealt with the static and seismic analyses of an historical masonry bridge placed in *Premilcuore*, a small village in Central Italy. The vulnerability analysis was tackled with several methods, considering both the traditional static approaches and the modern types of seismic analysis.

Considering the hypotheses, which are based on different structural aspects, it is very difficult to carry out a rational comparison of the numerical results. The different approach moreover produced different results that is hard to merge to a common factor.

However, the following conclusions can be drawn. As for the graphical methods, their graphical comparison shows that the values obtained using the Mèry's rule fall within the range identified with the Durand-Claye's method.

These methods show how the shape of the arch and the mechanical properties of the material are able to ensure the stability of the structure for the vertical loads considered above. In the analysis, the shear actions have been neglected. Therefore, the structure resulted to be safe under vertical gravitational loads.

With the purpose of analysing the bridge through other numerical methods, the non-linear kinematic analysis, based on rigid block model and limit analysis, the estimation of the collapse multiplier of the arch considered as set of rigid blocks was made. The analysis shows that the bridge arch, assumed subjected to inertial forces computed by the gravitational loads, is safe even with an elastic acceleration demand response spectrum. This aspect confirms the low vulnerability of these types of arch mechanisms to horizontal seismic actions, confirming

literature results. Finally, the *Premilcuore bridge* was subjected to a FEM sensitivity analysis considering three materials and two different models, for static and seismic actions.
The static analysis, with an incremental live load, allowed to evaluate the collapse factors. Both the load scenarios investigated are safe also considering precautionary hypotheses on the bridge material.
The seismic analysis identified the collapse loads and the most likely failure modes in presence of transverse seismic actions. The transverse direction is chosen here as complementary of the natural direction of kinematic analysis of the arch, in the transverse direction of the bridge. The more severe scenarios, approximately obtained in correspondence of the 80-90% of the design seismic actions, highlights a failure mode with a crushing on the foot of the foundation, with a mechanism that recalls to an incipient overturning of the bridge.
Summarizing, a comparison of the different methods, highlights that the bridge is structurally safe from a static point of view, as confirmed by FE analysis and graphical methods, whereas it presents some critical vulnerabilities in case of seismic actions acting along the river direction when FE models are adopted.

6 ACKNOWLEDGEMENTS

The financial support is also given by Region Sardinia (RICRAS-CTC/2018 and RAS L.R. 7/2007) and by the project “Monitoring of the structural and energy behavior of the existing constructions” that is acknowledged by Mario Lucio Puppio.

7 REFERENCES

[1] Page, J. (1993). *Masonry Arch Bridges*, London

[2] Bićanić, N.; Stirling, C.; Pearce, C. J. (2003). Discontinuous modelling of masonry bridges, *Computational Mechanics*, Vol. 31, No. 1, 60–68. doi:10.1007/s00466-002-0393-0

[3] Thavalingam, A.; Bicanic, N.; Robinson, J. I.; Ponniah, D. A. (2001). Computational framework for discontinuous modelling of masonry arch bridges, *Computers & Structures Structures*, Vol. 79, No. 19, 1821–1830. doi:10.1016/S0045-7949(01)00102-X

[4] Stochino, F.; Fadda, M. L.; Mistretta, F. (2018). Low cost condition assessment method for existing RC bridges, *Engineering Failure Analysis*, Vol. 86, 56–71. doi:10.1016/j.engfailanal.2017.12.021

[5] Oliveira, D. V; Lourenço, P. B.; Lemos, C. (2010). Geometric issues and ultimate load capacity of masonry arch bridges from the northwest Iberian Peninsula, *Engineering Structures*, Vol. 32, No. 12, 3955–3965. doi:https://doi.org/10.1016/j.engstruct.2010.09.006

[6] Mistretta, F.; Sanna, G.; Stochino, F.; Vacca, G. (2019). Structure from motion point clouds for structural monitoring, *Remote Sensing*, Vol. 11, No. 16. doi:10.3390/rs11161940

[7] Solla, M.; Lorenzo, H.; Riveiro, B.; Rial, F. I. (2011). Non-destructive methodologies in the assessment of the masonry arch bridge of Traba, Spain, *Engineering Failure Analysis*, Vol. 18, No. 3, 828–835. doi:https://doi.org/10.1016/j.engfailanal.2010.12.009

[8] Puppio, M. L.; Giresini, L. (2019). Estimation of tensile mechanical parameters of

existing masonry through the analysis of the collapse of Volterra's urban walls, *Frattura Ed Integrita Strutturale*, Vol. 13, No. 49, 725–738. doi:10.3221/IGF-ESIS.49.65

[9] Croce, P.; Landi, F.; Formichi, P. (2019). Probabilistic Seismic Assessment of Existing Masonry Buildings, *Buildings*, Vol. 9, No. 12. doi:10.3390/buildings9120237

[10] Lubowiecka, I.; Arias, P.; Riveiro, B.; Solla, M. (2011). Multidisciplinary approach to the assessment of historic structures based on the case of a masonry bridge in Galicia (Spain), *Computers & Structures*, Vol. 89, No. 17, 1615–1627. doi:https://doi.org/10.1016/j.compstruc.2011.04.016

[11] Beconcini, M. L.; Cioni, P.; Croce, P.; Formichi, P.; Landi, F.; Mochi, C. (2018). Non-linear static analysis of masonry buildings under seismic actions, *IMSCI 2018 - 12th International Multi-Conference on Society, Cybernetics and Informatics, Proceedings* (Vol. 1), 126–131

[12] Conde, B.; Ramos, L. F.; Oliveira, D. V; Riveiro, B.; Solla, M. (2017). Structural assessment of masonry arch bridges by combination of non-destructive testing techniques and three-dimensional numerical modelling: Application to Vilanova bridge, *Engineering Structures*, Vol. 148, 621–638. doi:https://doi.org/10.1016/j.engstruct.2017.07.011

[13] Casas, J. R. (2011). Reliability-based assessment of masonry arch bridges, *Construction and Building Materials*, Vol. 25, No. 4, 1621–1631. doi:https://doi.org/10.1016/j.conbuildmat.2010.10.011

[14] Zampieri, P.; Zanini, M. A.; Faleschini, F. (2016). Derivation of analytical seismic fragility functions for common masonry bridge types: methodology and application to real cases, *Engineering Failure Analysis*, Vol. 68, 275–291. doi:https://doi.org/10.1016/j.engfailanal.2016.05.031

[15] Foce, F.; Aita, D. (2003). The masonry arch between «limit» and «elastic» analysis. A critical re-examination of Durand-Claye's method, F. D. S.Huert, Madrid: I. Juan de Herrera, SEdHC, ETSAM, A.E. Benvenuto, COAM (Ed.), *First International Congress on Construction History (Madrid, 20th-24th January 2003)*, Madrid, Spain

[16] Solarino, F.; Oliveira, D.; Giresini, L. (2019). Wall-to-horizontal diaphragm connections in historical buildings: A state-of-the-art review, *Engineering Structures*, Vol. 199

[17] De Falco, A.; Giresini, L.; Sassu, M. (2013). Temporary preventive seismic reinforcements on historic churches: numerical modeling of San Frediano in Pisa, *Applied Mechanics and Materials*, Vol. 352

[18] Andreini, M.; De Falco, A.; Giresini, L.; Sassu, M. (2013). Collapse of the historic city walls of Pistoia (Italy): Causes and possible interventions, *Applied Mechanics and Materials*, Vols 351–352

[19] Alecci, V.; Barducci, S.; D'Ambrisi, A.; Stefano, M. De; Focacci, F.; Luciano, R.; Penna, R. (2019). Shear capacity of masonry panels repaired with composite materials: Experimental and analytical investigations, *Composites Part B: Engineering*, Vol. 171, 61–69. doi:https://doi.org/10.1016/j.compositesb.2019.04.013

[20] Sara, B.; Valerio, A.; Mario, D. S.; Giulia, M.; Luisa, R.; Gianfranco, S. (2020). Experimental and Analytical Investigations on Bond Behavior of Basalt-FRCM

Systems, *Journal of Composites for Construction*, Vol. 24, No. 1, 4019055. doi:10.1061/(ASCE)CC.1943-5614.0000985

[21] Giresini, L.; Puppio, M. L.; Taddei, F. (2020). Experimental pull-out tests and design indications for strength anchors installed in masonry walls, *Materials and Structures*, Vol. 53, No. 4, 103. doi:10.1617/s11527-020-01536-2

[22] NZSEE. (2017). New Zealand Society for Earthquake Engineering, Section C8: Unreinforced masonry buildings Part C – Detailed Seismic Assessment

[23] Casapulla, C.; Giresini, L.; Lourenço, P. B. (2017). Rocking and kinematic approaches for rigid block analysis of masonry walls: State of the art and recent developments, *Buildings*, Vol. 7, No. 3. doi:10.3390/buildings7030069

[24] Casapulla, C. (2008). Lower and upper bounds in closed form for out-of-plane strength of masonry structures with frictional resistances, F. E. D'Ayala D. (Ed.), *SAHC08-Structural Analysis of Historic Constructions*, Bath, 1191–1198

[25] Casapulla, C.; Argiento, L. U.; Maione, A.; Speranza, E. (2021). Upgraded formulations for the onset of local mechanisms in multi-storey masonry buildings using limit analysis, *Structures*

[26] Casapulla, C.; Maione, A.; Argiento, L. U.; Speranza, E. (2018). Corner failure in masonry buildings: An updated macro-modeling approach with frictional resistances, *European Journal of Mechanics, A/Solids*, Vol. 70, 213–225. doi:10.1016/j.euromechsol.2018.03.003

[27] Casapulla, C.; Maione, A.; Argiento, L. U. (2017). Seismic analysis of an existing masonry building according to the multi-level approach of the italian guidelines on cultural heritage, *Ingegneria Sismica*, Vol. 34, No. 1, 40–59

[28] Casapulla, C.; Argiento, L. U.; Maione, A. (2018). Seismic safety assessment of a masonry building according to Italian Guidelines on Cultural Heritage: simplified mechanical-based approach and pushover analysis, *Bulletin of Earthquake Engineering*, Vol. 16, No. 7, 2809–2837

[29] Casapulla, C.; Portioli, F.; Maione, A.; Landolfo, R. (2013). A macro-block model for in-plane loaded masonry walls with non-associative Coulomb friction, *Meccanica*, Vol. 48, No. 9, 2107–2126. doi:10.1007/s11012-013-9728-5

[30] Casapulla, C.; Portioli, F. (2016). Experimental tests on the limit states of dry-jointed tuff blocks, *Materials and Structures/Materiaux et Constructions*, Vol. 49, No. 3, 751–767. doi:10.1617/s11527-015-0536-3

[31] Giresini, L. (2017). Design strategy for the rocking stability of horizontally restrained masonry walls, M. F. M. Papadrakakis (Ed.), *COMPDYN 2017 - Proceedings of the 6th International Conference on Computational Methods in Structural Dynamics and Earthquake Engineering* (Vol. 2), Rhodes Island, Greece, 2963–2979. doi:10.7712/120117.5620.18188

[32] Giresini, L.; Solarino, F.; Paganelli, O.; Oliveira, D. V.; Froli, M. (2019). One-sided rocking analysis of corner mechanisms in masonry structures: influence of geometry, energy dissipation, boundary conditions, *Soil Dynamics and Earthquake Engineering*, in press

[33] Casapulla, C.; Giresini, L.; Argiento, L. U.; Maione, A. (2019). Nonlinear Static and

Dynamic Analysis of Rocking Masonry Corners Using Rigid Macro-Block Modeling, *International Journal of Structural Stability and Dynamics*, Vol. 19, No. 11, 1950137. doi:10.1142/S0219455419501372

[34] Giresini, L.; Taddei, F.; Casapulla, C.; Mueller, G. (2019). Stochastic assessment of rocking masonry façades under real seismic records, *COMPDYN 2019 7th ECCOMAS Thematic Conference on Computational Methods in Structural Dynamics and Earthquake Engineering*, Crete; Greece; 24th-26th June 2019, 673–689

[35] Solarino, F.; Giresini, L. (2021). Seismic vulnerability of rocking walls restrained with elasto-plastic ties, *Earthquake Eng. Struct. Dyn. (Submitted To)*

[36] Froli, M.; Giresini, L.; Laccone, F. (2019). Dynamics of a new seismic isolation device based on tribological smooth rocking (TROCKSISD), *Engineering Structures*, Vol. 193, 154–169

[37] Giresini, L.; Solarino, F.; Taddei, F.; Mueller, G. (2021). Experimental estimation of energy dissipation in rocking masonry walls restrained by an innovative seismic dissipator (LICORD), *Bulletin of Earthquake Engineering*. doi:10.1007/s10518-021-01056-6

[38] DeJong, M. J.; De Lorenzis, L.; Adams, S.; Ochsendorf, J. A. (2008). Rocking Stability of Masonry Arches in Seismic Regions, *Earthquake Spectra*, Vol. 24, No. 4, 847–865. doi:10.1193/1.2985763

[39] Decreto Ministeriale 17/01/2018. (2018). Italian Technical Standards for buildings (Nuove Norme Tecniche per le Costruzioni, in italian)

[40] Ministero delle infrastrutture e dei trasporti. Circolare 21 gennaio 2019, n. 7 Istruzioni per l'applicazione dell'«Aggiornamento delle "Norme tecniche per le costruzioni"», , 35 Gazzetta Ufficiale della Repubblica Italiana 1–337 (2019), 1–337

[41] Chácara, C.; Cannizzaro, F.; Pantò, B.; Caliò, I.; Lourenço, P. B. (2019). Seismic vulnerability of URM structures based on a Discrete Macro-Element Modeling (DMEM) approach, *Engineering Structures*, Vol. 201, 109715. doi:https://doi.org/10.1016/j.engstruct.2019.109715

[42] Caddemi, S.; Caliò, I.; Cannizzaro, F.; Pantò, B. (2017). New Frontiers on Seismic Modeling of Masonry Structures, *Frontiers in Built Environment*, Vol. 3, 39. doi:10.3389/fbuil.2017.00039

[43] Giresini, L.; Pantò, B.; Caddemi, S.; Caliò, I. (2019). Out-of-plane seismic response of masonry façades using discrete macro-element and rigid block models, *COMPDYN 2019 7th ECCOMAS Thematic Conference on Computational Methods in Structural Dynamics and Earthquake Engineering*, Crete; Greece; 24th-26th June 2019, 702–717

[44] Giresini, L. (2016). Energy-based method for identifying vulnerable macro-elements in historic masonry churches, *Bulletin of Earthquake Engineering*, Vol. 14, No. 3, 919–942. doi:10.1007/s10518-015-9854-7

[45] Caddemi, S.; Caliò, I.; Cannizzaro, F.; D'Urso, D.; Occhipinti, G.; Pantò, B.; Zurlo, R. (2018). A 'parsimonious' 3D Discrete Macro-Element Method for masonry arch bridges, *10th International Masonry Conference, G. Milani, A. Taliercio and S. Garrity (Eds.), Milan, Italy*

[46] Caddemi, S.; Caliò, I.; Cannizzaro, F.; D'Urso, D.; Pantò, B.; Rapicavoli, D.;

Occhipinti, G. (2019). 3D discrete macro-modelling approach for masonry arch bridges, *IABSE Symposium*

[47] Gönen, S.; Soyöz, S. (2021). Seismic analysis of a masonry arch bridge using multiple methodologies, *Engineering Structures*, Vol. 226, 111354. doi:https://doi.org/10.1016/j.engstruct.2020.111354

[48] Zampieri, P.; Perboni, S.; Tetougueni, C. D.; Pellegrino, C. (2020). Different Approaches to Assess the Seismic Capacity of Masonry Bridges by Non-linear Static Analysis, *Frontiers in Built Environment*, Vol. 6, 47. doi:10.3389/fbuil.2020.00047

[49] Pavan, M. (2012). *Ponti Della Romagna. Un Tesoro Nascosto*, Il Ponte Vecchio

[50] Pucci, A.; Sousa, H. S.; Puppio, M. L.; Giresini, L.; Matos, J. C.; Sassu, M. (2019). Method for sustainable large-scale bridge survey.pdf, *Towards a Resilient Built Environment Risk and Asset Management*, IABSE, Zurich, 1034–1041

[51] Campanella, G. (1928). *Trattato Generale Teorico Pratico Dell'arte Dell'ingegnere Civile, Industriale Ed Architetto: Ponti in Muratura*, Vallardi, Milano

[52] Campanella, G. (n.d.). *Masonry Bridges for Engineers*, Biblioteca Tecnica Internazionale, Milano

[53] Heyman, J. (1966). The stone skeleton, *International Journal of Solids and Structures*, Vol. 2, No. 2, 249–279. doi:10.1016/0020-7683(66)90018-7

[54] Borri, A.; De Maria, A. (2019). Il metodo IQM per la stima delle caratteristiche meccaniche delle murature : allineamento alla circolare n. 7/2019, ANIDIS (Ed.), *XVIII Congresso Nazionale "L'ingegneria Sismica in Italia", Ascoli Piceno 15-19 Settembre 2019*, Ascoli Piceno, 3–21

[55] D.M. 17/01/2018. (2018). Aggiornamento delle 'Norme Tecniche per le Costruzioni' (in italian)

[56] Puppio, M. L.; Giresini, L.; Doveri, F.; Sassu, M. (2019). Structural irregularity: The analysis of two reinforced concrete (r.c.) buildings, Vol. 7. doi:10.5267/j.esm.2018.12.002

[57] Parisi, F.; Augenti, N. (2012). Uncertainty in Seismic Capacity of Masonry Buildings, *Buildings*, Vol. 2, No. 3, 218–230. doi:10.3390/buildings2030218

[58] Puppio, M. L.; Pellegrino, M.; Giresini, L.; Sassu, M. (2017). Effect of material variability and mechanical eccentricity on the seismic vulnerability assessment of reinforced concrete buildings, *Buildings*, Vol. 7, No. 3. doi:10.3390/buildings7030066

[59] Torre, C. (2003). *Ponti in Muratura. Dizionario Storico-Tecnologico*, Alinea Editrice, Firenze

[60] CNR - Commissione di studio per la predisposizione e l'analisi di norme tecniche relative alle costruzioni. (2015). CNR-DT 213/2015 - Istruzioni per la Valutazione della Sicurezza Strutturale di Ponti Stradali in Muratura, Roma

[61] Clemente, P. (1997). *La Verifica Degli Archi a Conci Lapidei*, ENEA, Unità comunicazione e informazione